RESEARCH ARTICLE | OCTOBER 16 2024

Semiclassical perturbations of single-degree–of–freedom Hamiltonian systems I: Separatrix splitting

Tomoki Ohsawa ; Kazuyuki Yagasaki

J. Math. Phys. 65, 102706 (2024)
https://doi.org/10.1063/5.0198420

Journal of Mathematical Physics ARTICLE pubs.aip.org/aip/jmp

Semiclassical perturbations of single-degree–of–freedom Hamiltonian systems I: Separatrix splitting

Cite as: J. Math. Phys. 65, 102706 (2024); doi: 10.1063/5.0198420
Submitted: 18 January 2024 • Accepted: 13 September 2024 •
Published Online: 16 October 2024

Tomoki Ohsawa[1,a] and Kazuyuki Yagasaki[2,b]

AFFILIATIONS

[1] Department of Mathematical Sciences, The University of Texas at Dallas, 800 W Campbell Rd., Richardson, Texas 75080-3021, USA
[2] Department of Applied Mathematics and Physics, Graduate School of Informatics, Kyoto University, Yoshida-Honmachi, Sakyo-ku, Kyoto 606-8501, Japan

[a] E-mail: tomoki@utdallas.edu
[b] Author to whom correspondence should be addressed: yagasaki@amp.i.kyoto-u.ac.jp

ABSTRACT

We study semiclassical perturbations of single-degree-of-freedom Hamiltonian systems possessing hyperbolic saddles with homoclinic orbits, and provide a sufficient condition for the separatrices to split, using a Melnikov-type approach. The semiclassical systems give approximations of the expectation values of the positions and momenta to the semiclassical Schrödinger equations with Gaussian wave packets as the initial conditions. The occurrence of separatrix splitting explains a mechanism for the existence of trajectories to cross the separatrices on the classical phase plane in the expectation value dynamics. Such separatrix splitting does not occur in standard systems of Hagedorn and Heller for the semiclassical Gaussian wave packet dynamics as well as in the classical systems. We illustrate our theory for the potential of a simple pendulum and give numerical computations for the stable and unstable manifolds in the semiclassical system as well as solutions crossing the separatrices.

I. INTRODUCTION

Consider the initial value problem of the Schrödinger equation,

$$\begin{aligned} &\mathrm{i}\,\varepsilon\frac{\partial}{\partial t}\psi(t,x) = \hat{H}\psi(t,x) \quad \text{with } \hat{H} := \frac{1}{2}\hat{p}^2 + V(x), \\ &\psi(0,x) = \phi_0(q(0),p(0),Q(0),P(0),S(0);x), \end{aligned} \tag{1.1}$$

where $(t,x) \in \mathbb{R}\times\mathbb{R}$; ε is the semiclassical parameter such that $0<\varepsilon\ll 1$; $V(x)$ is a scalar function; $\hat{p} := -\mathrm{i}\varepsilon\partial/\partial x$ is the momentum operator; and ϕ_0 is the Gaussian wave function

$$\phi_0(q,p,Q,P,S;x) := \frac{Q^{-1/2}}{(\pi\varepsilon)^{1/4}}\exp\left\{\frac{\mathrm{i}}{\varepsilon}\left(\frac{1}{2}PQ^{-1}(x-q)^2 + p(x-q) + S\right)\right\}. \tag{1.2}$$

In addition, we assume the following on the potential $V(x)$:

(A1). $V(x)$ is C^4 and bounded from below and its second derivative $V''(x)$ is bounded.

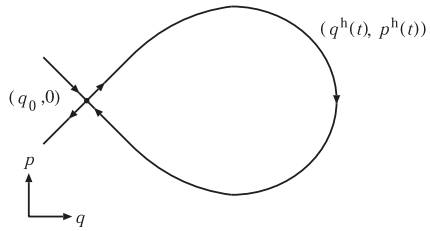

FIG. 1. Assumption (A2).

The parameters (q,p) live in the cotangent bundle $T^*\mathbb{R} \cong \mathbb{R}\times\mathbb{R}$. We note in passing that both x and q denote positions. The variable x and the position operator $\hat{x}$ are associated with the spatial variable for the Schrödinger equation (1.1), whereas q denotes the (time-dependent) position in the classical sense. The parameter $S \in \mathbb{R}$ is a phase factor, whereas $Q = Q_1 + \mathrm{i}Q_2, P = P_1 + \mathrm{i}P_2 \in \mathbb{C}$ satisfy

$$Q^*P - P^*Q = 2\mathrm{i} \iff \begin{bmatrix} Q_1 & Q_2 \\ P_1 & P_2 \end{bmatrix} \in \mathsf{Sp}(2,\mathbb{R}) = \mathsf{SL}(2,\mathbb{R}), \tag{1.3}$$

which also ensures that PQ^{-1} is in the upper-half space of $\mathbb{C}$, i.e., $\mathrm{Im}(PQ^{-1}) = |Q|^{-2} > 0$ so that $\phi_0 \in L^2(\mathbb{R})$. See, e.g., [Ref. 17, lemma V.1.1]. Exact solutions to the initial value problem of (1.1) can be obtained only for special cases of $V(x)$ (see, e.g., Ref. 2).

The corresponding classical Hamiltonian system is written as

$$\dot{q} = p, \quad \dot{p} = -V'(q), \quad (q,p) \in \mathbb{R}\times\mathbb{R}, \tag{1.4}$$

where the dot represents differentiation with respect to t and the Hamiltonian is given by

$$H_0(q,p) := \frac{1}{2}p^2 + V(q).$$

It is a well-known fact that such a single-degree-of-freedom Hamiltonian system (1.4) is generally integrable:[3,21] Its solutions can be obtained by quadrature, in contrast to (1.1). We assume the following on (1.4):

(A2). There exists a hyperbolic saddle at $(q,p) = (q_0,0)$ to which there exists a homoclinic orbit $(q^{\mathrm{h}}(t),p^{\mathrm{h}}(t))$ (see Fig. 1).

Assumption (A2) means that the saddle $(q_0,0)$ has one-dimensional stable and unstable manifolds that coincide along the homoclinic orbit acting as a separatrix. Henceforth we assume that $p^{\mathrm{h}}(0) \neq 0$ without loss of generality. Indeed, we only have to shift the variable t otherwise. Our special attention is paid to the potential

$$V(q) = -\cos q, \tag{1.5}$$

for which Eq. (1.4) represents the classical dynamics of a simple pendulum.

Let $\hat{x}$ be the position operator and let $\hat{p}$ be the momentum operator as introduced above. We consider the trajectory of their expectation values, i.e., $(\langle\hat{x}\rangle(t),\langle\hat{p}\rangle(t))$ with

$$\langle\hat{x}\rangle(t) := \langle\psi(t),\hat{x}\,\psi(t)\rangle, \qquad \langle\hat{p}\rangle(t) := \langle\psi(t),\hat{p}\,\psi(t)\rangle$$

in the classical phase space $T^*\mathbb{R} = \mathbb{R}\times\mathbb{R}$, where we have used the shorthand $\psi(t) := \psi(t,\cdot) \in L^2(\mathbb{R})$ for the exact solution to the initial value problem (1.1). Note that $(\langle\hat{x}\rangle(0),\langle\hat{p}\rangle(0)) = (q(0),p(0))$ because we assume the Gaussian (1.2) at $t = 0$. We want to see how the trajectory $(\langle\hat{x}\rangle(t),\langle\hat{p}\rangle(t))$ deviates from the classical solution $(q(t),p(t))$ to (1.4) in the semiclassical regime.

In the formal classical limit $\varepsilon \to 0$, the above expectation value dynamics (EVD) coincides with the dynamics of the classical Hamiltonian system (1.4) in the sense that $(\langle\hat{x}\rangle(t),\langle\hat{p}\rangle(t)) = (q(t),p(t))$. In particular, none of the trajectories in (1.4) crosses the separatrix $\Gamma = \{(q^{\mathrm{h}}(t),p^{\mathrm{h}}(t)) \mid t \in \mathbb{R}\} \cup \{(q_0,0)\}$. We note that, even when $\varepsilon > 0$, if the potential V is quadratic, then we have $(\langle\hat{x}\rangle(t),\langle\hat{p}\rangle(t)) = (q(t),p(t))$ again. See Refs. 11, 12, and 14 for the details. When $\varepsilon > 0$ and the potential V is not quadratic, the EVD is no longer expected to be governed by the classical Hamiltonian system (1.4).

We consider (1.5) as an example of non-quadratic potentials, and take $\mathbb{S}^1 = \mathbb{R}/2\pi\mathbb{Z}$ as the configuration space, so that the two orbits acting as the separatrices become homoclinic orbits. Figure 2 shows a numerically computed EVD for $\varepsilon = 0.1$ and $(q(0),p(0),Q(0),P(0),S(0)) = (0,1.95,-1.396\,42 + \mathrm{i},1,0)$. Here we used Egorov's method [6,15,16] or the Initial Value Representation (IVR) method,[18–20,28] which is known to give an $O(\varepsilon^2)$ approximation to the exact EVD $t \mapsto (\langle\hat{x}\rangle(t),\langle\hat{p}\rangle(t))$ [see, e.g., Refs. 4 and 9 and (Ref. 31, Chap. 11)], with 10^6 sample initial values. We observe that the trajectory passes through the separatrix outward. This suggests that the separatrix is breaking up in the semiclassical regime due to quantum effects. We want to quantify the effect of the semiclassical parameter ε to the breakup.

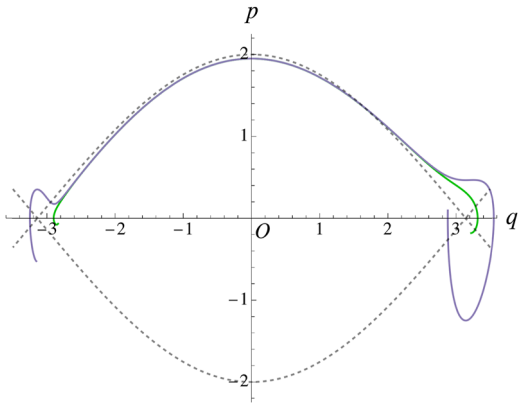

FIG. 2. Approximate EVD $t \mapsto (\langle\hat{x}\rangle(t), \langle\hat{p}\rangle(t))$ for $-5 \le t \le 5$ computed by Egorov's method for the initial value problem of the Schrödinger equation (1.1) with the potential (1.5) for $\varepsilon = 0.1$ and $(q(0), p(0), Q(0), P(0), S(0)) = (0, 1.95, -1.396\,42 + \mathrm{i}, -1, 0)$. The green curve represents the numerical result. The purple curve represents the (q,p)-components of a numerical solution to the semiclassical system (1.6) with the same initial condition. The dashed curves represent the separatrices in the classical system (1.4).

To this end, we employ an approximate approach proposed in Refs. 25 and 26 for the EVD. Specifically, consider the semiclassical dynamics

$$\begin{aligned} &\dot{q} = p, \quad \dot{p} = -V'(q) - \frac{1}{4}\varepsilon(Q_1^2 + Q_2^2)V'''(q), \\ &\dot{Q}_j = P_j, \quad \dot{P}_j = -V''(q)Q_j, \quad j = 1, 2. \end{aligned} \tag{1.6}$$

with the same initial $(q(0), p(0), Q(0), P(0))$ as in (1.1). It was shown in Ref. 25 under assumption (A1) that the (q,p)-components of the solution to (1.6) approximate the exact expectation value $(\langle\hat{x}\rangle(t), \langle\hat{p}\rangle(t))$ of the initial value problem (1.1) in the sense that $q(t) - \langle\hat{x}\rangle(t)$ and $p(t) - \langle\hat{p}\rangle(t)$ are both $O(\varepsilon^{3/2})$.

We note that the $O(\varepsilon)$ correction term in (1.6) is the only difference from the equations of Hagedorn[11,12] and Heller,[14]

$$\dot{q} = p, \quad \dot{p} = -V'(q), \quad \dot{Q}_j = P_j, \quad \dot{P}_j = -V''(q)Q_j, \quad j = 1, 2, \tag{1.7}$$

which give an $O(\varepsilon)$ approximation to the exact EVD as opposed to $O(\varepsilon^{3/2})$ under assumption (A1). See Ref. 25 for the details. We refer to (1.7) as the unperturbed system below. In addition, the correction term renders the system (1.6) a Hamiltonian system on $T^*\mathbb{R} \times \mathbb{C}^2$ with the symplectic form

$$\Omega^\varepsilon := \mathrm{d}q \wedge \mathrm{d}p + \frac{1}{2}\varepsilon \sum_{j=1}^{2} (\mathrm{d}Q_j \wedge \mathrm{d}P_j)$$

and the Hamiltonian

$$H^\varepsilon(q, p, Q, P) := H_0(q, p) + \varepsilon H_1(q, p, Q, P),$$

where

$$H_1(q, p, Q, P) := \frac{1}{4}(P_1^2 + P_2^2 + (Q_1^2 + Q_2^2)V''(q)).$$

We remark that Eq. (1.7) consists of the classical Hamiltonian system (1.4) and its variational equation, hence having no semiclassical corrections. However, Hagedorn[11,12] used the time-dependent Gaussian $\phi(t) := \phi_0(q(t), p(t), Q(t), P(t), S(t);\, x)$ along the solution of (1.7) and proved that $\phi(t)$ gives an $O(\varepsilon^{1/2})$ approximation in L^2-norm to the exact solution $\psi(t)$ of (1.1). Moreover, it was shown in Refs. 5, 7, and 24 that the variational equations of the classical systems and their fundamental matrices, which are often referred to as the *Jacobi equations* and *matrices*, respectively, can play an important role in computation of the semiclassical propagators by the Feynman path integral technique.[10] Some interesting results in a new direction related to this approach based on the Feynman integrals have recently been reported in Refs. 1 and 22. See also Remark 2.3.

The (q,p)-components of a numerical solution to (1.6) with (1.5) for $\varepsilon = 0.1$ under the initial condition

$$(q(0), p(0), Q_1(0), Q_2(0), P_1(0), P_2(0)) = (0, 1.95, -1.396\,42, 1, -1, 0)$$

on the time interval $[-5, 5]$ is displayed in Fig. 2. The value for $Q_1(0)$ was chosen so that the Hamiltonian becomes $H^\varepsilon = 1$ given the other initial values. We observe that they pass through the separatrix like the approximate EVD, although not only outward but also inward. Thus,

the semiclassical system (1.6) can capture the separatrix crossing in the EVD for (1.1). Our objective of this paper is to explain the mechanism for separatrix crossing in (1.6), which never occurs in the classical system (1.4) and the unperturbed system (1.7) since $H_0(q,p)$ is conserved.

First, we easily see that both (1.6) and (1.7) have a hyperbolic saddle

$$(q,p,Q,P) = (q_0,0,0,0) \in \mathbb{R}\times\mathbb{R}\times\mathbb{R}^2\times\mathbb{R}^2 \tag{1.8}$$

which has three-dimensional stable and unstable manifolds, where we have identified $\mathbb{C}$ with $\mathbb{R}^2$. Let $W^{\mathrm{s}}_\varepsilon$ and $W^{\mathrm{u}}_\varepsilon$ denote its three-dimensional stable and unstable manifolds in (1.6). So W^{s}_0 and W^{u}_0 represent its three-dimensional stable and unstable manifolds in (1.7). The manifolds W^{s}_0 and W^{u}_0 coincide along a three-dimensional manifold $\mathscr{M}$ intersecting the (q,p)-plane in Γ, as shown below (see Proposition 2.2). This also implies that the system (1.7) has no trajectory of which the (q,p)-components cross the separatrix Γ.

We now state our main result as follows.

Theorem 1.1. *Suppose that assumptions (A1) and (A2) hold and*

$$\int_{-\infty}^{\infty} p^{\mathrm{h}}(t)^2\dot{p}^{\mathrm{h}}(t)V'''(q^{\mathrm{h}}(t))\mathrm{d}t \neq 0. \tag{1.9}$$

Then for $\varepsilon>0$ sufficiently small, the stable and unstable manifolds, $W^{\mathrm{s}}_\varepsilon$ and W^{u}_ε, of the hyperbolic saddle (1.8) split and their distance is $O(\varepsilon)$ outside of the (q,p)-plane. Moreover, their distance is $O(\varepsilon)$ in the directions

$$(q,p,Q_1,Q_2,P_1,P_2) = (0,0,\dot{p}^{\mathrm{h}}(t_0),0,-p^{\mathrm{h}}(t_0),0) \tag{1.10}$$

and

$$(q,p,Q_1,Q_2,P_1,P_2) = (0,0,0,\dot{p}^{\mathrm{h}}(t_0),0,-p^{\mathrm{h}}(t_0)) \tag{1.11}$$

while it is at most $O(\varepsilon^2)$ in the direction

$$(q,p,Q_1,Q_2,P_1,P_2) = (V'(q^{\mathrm{h}}(t_0)),p^{\mathrm{h}}(t_0),0,0,0,0), \tag{1.12}$$

near the point

$$\begin{aligned}&(q,p,Q_1,Q_2,P_1,P_2)\\ &= (q^{\mathrm{h}}(t_0),p^{\mathrm{h}}(t_0),\beta_1 p^{\mathrm{h}}(t_0),\beta_2 p^{\mathrm{h}}(t_0),\beta_1\dot{p}^{\mathrm{h}}(t_0),\beta_2\dot{p}^{\mathrm{h}}(t_0))\end{aligned} \tag{1.13}$$

for any $t_0\in\mathbb{R}$ and $\beta=(\beta_1,\beta_2)\in\mathbb{R}^2\backslash\{0\}$.

A proof of Theorem 1.1 is given in Sec. III. It is essential in the proof to use modifications of the arguments, including a Melnikov-type approach, in the proof of Theorem 4.1 of Ref. 29.

Remark 1.2.

(i) *The stable and unstable manifolds, $W^{\mathrm{s}}_\varepsilon$ and $W^{\mathrm{u}}_\varepsilon$, intersect the (q,p)-plane in $\Gamma\backslash\{(q_0,0)\}$, i.e., they coincide on the (q,p)-plane, even for $\varepsilon>0$.*

(ii) *The point (1.13) lies on the three-dimensional manifold $\mathscr{M}$ and the directions (1.10)–(1.12) are normal to $\mathscr{M}$ there.*

Thus, when $\varepsilon>0$ is sufficiently small but positive, if condition (1.9) holds, then $W^{\mathrm{s}}_\varepsilon$ and $W^{\mathrm{u}}_\varepsilon$ split so that the system (1.6) has trajectories of which the (q,p)-components cross the separatrix Γ as in Fig. 2, in contrast to (1.7). This result suggests the system (1.6) is not integrable if condition (1.9) holds. This topic will be discussed in the companion paper.[30]

The outline of this paper is as follows. We describe the phase space structure of (1.7) in Sec. II and give a proof of Theorem 1.1 in Sec. III. Finally, we illustrate the main result for the semiclassical system (1.6) with the potential (1.5) in Sec. IV.

II. UNPERTURBED PHASE SPACE

In this section, we describe the phase space structure of the unperturbed system (1.7). We begin with an auxiliary result.

The (Q_j,P_j)-components of (1.7) become

$$\dot{Q}_j = P_j,\quad \dot{P}_j = -V''(q^{\mathrm{h}}(t))Q_j \tag{2.1}$$

on $\mathscr{M}$ for $j=1,2$. We have the following on (2.1).

Lemma 2.1. Two linearly independent solutions of (2.1) are given by

$$(Q_j, P_j) = (p^{\mathrm{h}}(t), \dot{p}^{\mathrm{h}}(t)), (\chi(t), \dot{\chi}(t)),$$

where

$$\chi(t) := p^{\mathrm{h}}(t) \int_0^t \frac{\mathrm{d}\tau}{p^{\mathrm{h}}(\tau)^2}. \tag{2.2}$$

Proof. It is easy to see that $(Q_j, P_j) = (p^{\mathrm{h}}(t), \dot{p}^{\mathrm{h}}(t))$ is a solution to (2.1). Indeed, since by the second equation of (1.4) $\dot{p}^{\mathrm{h}}(t) = -V'(q^{\mathrm{h}}(t))$, we compute

$$\begin{aligned}\dot{P}_j = \ddot{p}^{\mathrm{h}}(t) &= -\frac{\mathrm{d}}{\mathrm{d}t} V'(q^{\mathrm{h}}(t)) = -V''(q^{\mathrm{h}}(t))\dot{q}^{\mathrm{h}}(t) \\ &= -V''(q^{\mathrm{h}}(t))p^{\mathrm{h}}(t) = -V''(q^{\mathrm{h}}(t))Q_j,\end{aligned}$$

while $\dot{Q}_j = \dot{p}^{\mathrm{h}}(t) = P_j$.

On the other hand, $Q_j = p^{\mathrm{h}}(t)$ is also a solution to the second-order differential equation

$$\ddot{Q}_j + V''(q^{\mathrm{h}}(t))Q_j = 0, \tag{2.3}$$

and another linearly independent solution can easily be obtained by variation of constants as follows. Substituting $Q_j = y(t)p^{\mathrm{h}}(t)$ into the above equation and using $\ddot{p}^{\mathrm{h}}(t) = -V''(q^{\mathrm{h}}(t))p^{\mathrm{h}}(t)$ again, we have

$$\ddot{y}p^{\mathrm{h}}(t) + 2\dot{y}\dot{p}^{\mathrm{h}}(t) = 0,$$

which is rewritten as

$$\frac{\ddot{y}}{\dot{y}} = -\frac{2\dot{p}^{\mathrm{h}}(t)}{p^{\mathrm{h}}(t)}$$

if $\dot{y} \neq 0$. Integrating the above equation, we compute

$$\log|\dot{y}| = -2\log|p^{\mathrm{h}}(t)| + \text{const.},$$

which yields

$$\dot{y} = \frac{C}{p^{\mathrm{h}}(t)^2},$$

where C is any nonzero constant. Thus we have $Q_j = \chi(t)$ as a particular solution to (2.3). Noting the first equation of (2.1), we obtain the desired result. □

We easily see that $\chi(t)$ is unbounded since $p^{\mathrm{h}}(t), \dot{p}^{\mathrm{h}}(t)$ tend to zero as $t \to \pm\infty$ and by L'Hôpital's rule

$$\lim_{t\to\pm\infty} \chi(t) = \lim_{t\to\pm\infty} \frac{\int_0^t \frac{\mathrm{d}\tau}{p^{\mathrm{h}}(\tau)^2}}{\frac{1}{p^{\mathrm{h}}(t)}} = -\lim_{t\to\pm\infty} \frac{\frac{1}{p^{\mathrm{h}}(t)^2}}{\frac{\dot{p}^{\mathrm{h}}(t)}{p^{\mathrm{h}}(t)^2}} = -\lim_{t\to\pm\infty} \frac{1}{\dot{p}^{\mathrm{h}}(t)} = \pm\infty.$$

Moreover,

$$(q, p, Q_1, Q_2, P_1, P_2) = (q^{\mathrm{h}}(t), p^{\mathrm{h}}(t), \beta_1 p^{\mathrm{h}}(t), \beta_2 p^{\mathrm{h}}(t), \beta_1 \dot{p}^{\mathrm{h}}(t), \beta_2 \dot{p}^{\mathrm{h}}(t)) \tag{2.4}$$

is a two-parameter family of homoclinic orbits to the hyperbolic saddle (1.8). Thus, we have the following.

Proposition 2.2. The hyperbolic saddle (1.8) has a three-dimensional homoclinic manifold,

$$\begin{aligned}\mathscr{M} = \{&(q, p, Q_1, Q_2, P_1, P_2) \\ &= (q^{\mathrm{h}}(t), p^{\mathrm{h}}(t), \beta_1 p^{\mathrm{h}}(t), \beta_2 p^{\mathrm{h}}(t), \beta_1 \dot{p}^{\mathrm{h}}(t), \beta_2 \dot{p}^{\mathrm{h}}(t)) \mid t \in \mathbb{R}, (\beta_1, \beta_2) \in \mathbb{R}^2\} \\ &\cup \{(q_0, 0, 0, 0, 0, 0)\},\end{aligned}$$

on which any trajectory converges to it as $t \to \pm\infty$, in the six-dimensional phase space of (1.7).

Note that the manifold $\mathscr{M}$ intersects the (q, p)-plane in Γ.

Remark 2.3. When a solution to the (q,p)-components of (1.7) is given, the (Q_j,P_j)-components of (1.7) are the same as a linear system called the variational equation of its (q,p)-components along the solution for $j=1,2$. Morales-Ruiz and Ramis[23] showed that if a (meromorphic) Hamiltonian system is integrable in the Liouville sense,[3,21] then its variational equation along any particular solution can be solved by quadrature. See also Ref. 21. This result provides a reason why the (Q_j,P_j)-components of (1.7) are solved by quadrature, as in Lemma 2.1, since single-degree-of-freedom Hamiltonian systems such as (1.4) are necessarily Liouville-integrable. Morales-Ruiz and his coworkers[1,22] also used this fact and analyzed semiclassical models derived by the WKB approximation[5,7,24] based on the Feynman path integrals[10] for Hamiltonian systems.

III. PROOF OF THEOREM 1.1

We turn to (1.6) with $\varepsilon>0$. Using arguments given in the proof of Theorem 4.1 of Ref. 29, especially a Melnikov-type approach, we estimate the distance between its stable and unstable manifolds, $W^{\rm s}_\varepsilon$ and $W^{\rm u}_\varepsilon$, and prove Theorem 1.1. Hamiltonian characters of (1.6) are not used in the proof.

Let

$$\begin{aligned}&(q,p,Q_1,Q_2,P_1,P_2)\\&=(q^{\rm h}(t),p^{\rm h}(t),\beta_1p^{\rm h}(t),\beta_2p^{\rm h}(t),\beta_1\dot p^{\rm h}(t),\beta_2\dot p^{\rm h}(t))\\&\quad+\varepsilon(\tilde q^{\rm s}(t;\beta,\varepsilon),\tilde p^{\rm s}(t;\beta,\varepsilon),\tilde Q_1^{\rm s}(t;\beta,\varepsilon),\tilde Q_2^{\rm s}(t;\beta,\varepsilon),\tilde P_1^{\rm s}(t;\beta,\varepsilon),\tilde P_2^{\rm s}(t;\beta,\varepsilon))\end{aligned}\tag{3.1}$$

and

$$\begin{aligned}&(q,p,Q_1,Q_2,P_1,P_2)\\&=(q^{\rm h}(t),p^{\rm h}(t),\beta_1p^{\rm h}(t),\beta_2p^{\rm h}(t),\beta_1\dot p^{\rm h}(t),\beta_2\dot p^{\rm h}(t))\\&\quad+\varepsilon(\tilde q^{\rm u}(t;\beta,\varepsilon),\tilde p^{\rm u}(t;\beta,\varepsilon),\tilde Q_1^{\rm u}(t;\beta,\varepsilon),\tilde Q_2^{\rm u}(t;\beta,\varepsilon),\tilde P_1^{\rm u}(t;\beta,\varepsilon),\tilde P_2^{\rm u}(t;\beta,\varepsilon))\end{aligned}\tag{3.2}$$

denote orbits on $W^{\rm s}_\varepsilon$ and $W^{\rm u}_\varepsilon$ for $t\in[0,\infty)$ and $(-\infty,0]$, respectively, for any $\beta=(\beta_1,\beta_2)\in\mathbb{R}^2\backslash\{0\}$. Take $t=t_0\in\mathbb{R}$ arbitrarily. We compute the distances between $W^{\rm s}_\varepsilon$ and $W^{\rm u}_\varepsilon$ near the point (1.13) in the directions (1.10)–(1.12). The distances are represented as

$$\begin{aligned}&d_0(t_0,\beta,\varepsilon)\\&=\varepsilon\frac{(V'(q^{\rm h}(t_0)),p^{\rm h}(t_0))}{|(V'(q^{\rm h}(t_0),p^{\rm h}(t_0))|}\cdot(\tilde q^{\rm u}(t_0;\beta,\varepsilon)-\tilde q^{\rm s}(t_0;\beta,\varepsilon),\tilde p^{\rm u}(t_0;\beta,\varepsilon)-\tilde p^{\rm s}(t_0;\beta,\varepsilon))\end{aligned}$$

for (1.12) and

$$\begin{aligned}&d_j(t_0,\beta,\varepsilon)\\&=\varepsilon\frac{(\dot p^{\rm h}(t_0),-p^{\rm h}(t_0))}{|(\dot p^{\rm h}(t_0),-p^{\rm h}(t_0))|}\cdot(\tilde Q_j^{\rm u}(t_0;\varepsilon)-\tilde Q_j^{\rm s}(t_0;\varepsilon),\tilde P_j^{\rm u}(t_0;\beta,\varepsilon)-\tilde P_j^{\rm s}(t_0;\beta,\varepsilon)),\quad j=1,2.\end{aligned}$$

for (1.10) and (1.11), where "$\cdot$" represents the dot product. See Fig. 3 for the definitions of $d_j(t_0,\beta,\varepsilon)$, $j=1,2$. The definition of $d_0(t_0,\beta,\varepsilon)$ is similar. Substituting (3.1) and (3.2) into (1.6), we obtain

$$\begin{aligned}&\dot{\tilde q}^{\rm s,u}(t;\beta,\varepsilon)=\tilde p^{\rm s,u}(t;\beta,\varepsilon),\\&\dot{\tilde p}^{\rm s,u}(t;\beta,\varepsilon)=-V''(q^{\rm h}(t))\tilde q^{\rm s,u}(t;\beta,\varepsilon)-\frac14(\beta_1^2+\beta_2^2)p^{\rm h}(t)^2V'''(q^{\rm h}(t))+O(\varepsilon),\\&\dot{\tilde Q}_j^{\rm s,u}(t;\beta,\varepsilon)=\tilde P_j^{\rm s,u}(t;\beta,\varepsilon),\\&\dot{\tilde P}_j^{\rm s,u}(t;\beta,\varepsilon)=-V''(q^{\rm h}(t))\tilde Q_j^{\rm s,u}(t;\beta,\varepsilon)-\beta_jV'''(q^{\rm h}(t))p^{\rm h}(t)\tilde q^{\rm s,u}(t;\beta,\varepsilon)+O(\varepsilon)\end{aligned}\tag{3.3}$$

for $j=1,2$, where the superscript "s" or "u" is taken simultaneously.

From Lemma 2.1 we see that

$$\Phi(t)=\begin{pmatrix}p^{\rm h}(t)&\chi(t)\\ \dot p^{\rm h}(t)&\dot\chi(t)\end{pmatrix}$$

is a fundamental matrix to the $(\tilde q^{\rm s,u},\tilde p^{\rm s,u})$-components of (3.3) having a coefficient matrix whose trace is zero. Since $\chi(0)=0$ and $\dot\chi(0)=1/p^{\rm h}(0)$ by

$$\dot\chi(t)=\dot p^{\rm h}(t)\int_0^t\frac{{\rm d}\tau}{p^{\rm h}(\tau)^2}+\frac{1}{p^{\rm h}(t)},$$

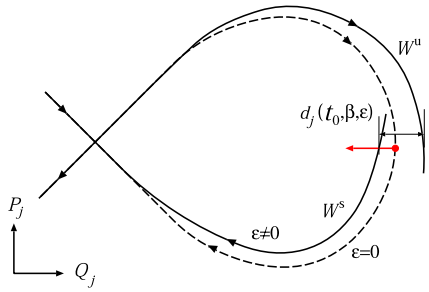

FIG. 3. Distances $d_j(t_0,\beta,\varepsilon)$, $j=1,2$, between the stable and unstable manifolds $W^{\mathrm{s}}_\varepsilon$ and $W^{\mathrm{u}}_\varepsilon$. The red disk and arrow, respectively, represent the point (1.13) and vector (1.10) or (1.11).

we have

$$\det\Phi(t)=\det\Phi(0)=1,$$

so that

$$\Phi(t)^{-1}=\begin{pmatrix}\dot\chi(t) & -\chi(t)\\ -\dot p^{\mathrm{h}}(t) & p^{\mathrm{h}}(t)\end{pmatrix}.$$

We have simple expressions for $\tilde q^{\mathrm{s}}(t;\beta,\varepsilon)$ and $\tilde q^{\mathrm{u}}(t;\beta,\varepsilon)$ as follows.

Lemma 3.1. We have

$$\tilde q^{\mathrm{s}}(t;\beta,\varepsilon)=\frac14(\beta_1^2+\beta_2^2)\dot p^{\mathrm{h}}(t)+O(\varepsilon),\quad \tilde q^{\mathrm{u}}(t;\beta,\varepsilon)=\frac14(\beta_1^2+\beta_2^2)\dot p^{\mathrm{h}}(t)+O(\varepsilon). \tag{3.4}$$

Proof. Noting that

$$\lim_{t\to\infty}(\tilde q^{\mathrm{s}}(t;\beta,\varepsilon),\tilde p^{\mathrm{s}}(t;\beta,\varepsilon)),\ \lim_{t\to-\infty}(\tilde q^{\mathrm{u}}(t;\beta,\varepsilon),\tilde p^{\mathrm{u}}(t;\beta,\varepsilon))=(0,0),$$

we solve the $(\tilde q^{\mathrm{s,u}},\tilde p^{\mathrm{s,u}})$-components of (3.3) to obtain

$$\begin{aligned}&\begin{pmatrix}\tilde q^{\mathrm{s}}(t;\beta,\varepsilon)\\ \tilde p^{\mathrm{s}}(t;\beta,\varepsilon)\end{pmatrix}\\ &=-\frac14(\beta_1^2+\beta_2^2)\Phi(t)\left(\int_t^\infty\begin{pmatrix}\chi(\tau)p^{\mathrm{h}}(\tau)^2V'''(q^{\mathrm{h}}(\tau))\\ -p^{\mathrm{h}}(\tau)^3V'''(q^{\mathrm{h}}(\tau))\end{pmatrix}\mathrm{d}\tau+\begin{pmatrix}\tilde q_0^{\mathrm{s}}\\ 0\end{pmatrix}\right),\\ &\begin{pmatrix}\tilde q^{\mathrm{u}}(t;\beta,\varepsilon)\\ \tilde p^{\mathrm{u}}(t;\beta,\varepsilon)\end{pmatrix}\\ &=\frac14(\beta_1^2+\beta_2^2)\Phi(t)\left(\int_{-\infty}^t\begin{pmatrix}\chi(\tau)p^{\mathrm{h}}(\tau)^2V'''(q^{\mathrm{h}}(\tau))\\ -p^{\mathrm{h}}(\tau)^3V'''(q^{\mathrm{h}}(\tau))\end{pmatrix}\mathrm{d}\tau+\begin{pmatrix}\tilde q_0^{\mathrm{u}}\\ 0\end{pmatrix}\right)\end{aligned} \tag{3.5}$$

up to $O(1)$, where $\tilde q_0^{\mathrm{s,u}}$ are arbitrary constants. Since

$$\ddot p^{\mathrm{h}}(t)=-V''(q^{\mathrm{h}}(t))\dot q^{\mathrm{h}}(t)=-V''(q^{\mathrm{h}}(t))p^{\mathrm{h}}(t) \tag{3.6}$$

and $p^{\mathrm{h}}(t),\dot p^{\mathrm{h}}(t)$ tend to zero as $t\to\pm\infty$, we have

$$\begin{aligned}&\frac{\mathrm{d}}{\mathrm{d}t}\left(p^{\mathrm{h}}(t)^2V''(q^{\mathrm{h}}(t))+\dot p^{\mathrm{h}}(t)^2\right)\\ &=p^{\mathrm{h}}(t)^3V'''(q^{\mathrm{h}}(t))+2p^{\mathrm{h}}(t)\dot p^{\mathrm{h}}(t)V''(q^{\mathrm{h}}(t))+2\dot p^{\mathrm{h}}(t)\ddot p^{\mathrm{h}}(t)\\ &=p^{\mathrm{h}}(t)^3V'''(q^{\mathrm{h}}(t)),\end{aligned} \tag{3.7}$$

so that

$$\begin{aligned}-\int_t^\infty p^{\mathrm{h}}(\tau)^3V'''(q^{\mathrm{h}}(\tau))\mathrm{d}t&=\int_{-\infty}^t p^{\mathrm{h}}(\tau)^3V'''(q^{\mathrm{h}}(\tau))\mathrm{d}\tau\\ &=p^{\mathrm{h}}(t)^2V''(q^{\mathrm{h}}(t))+\dot p^{\mathrm{h}}(t)^2.\end{aligned} \tag{3.8}$$

On the other hand, by (2.2) we have

$$\chi(t)p^{\mathrm{h}}(t)^2V'''(q^{\mathrm{h}}(t)) = p^{\mathrm{h}}(t)^3V'''(q^{\mathrm{h}}(t))\int_0^t \frac{\mathrm{d}\tau}{p^{\mathrm{h}}(\tau)^2},$$

which yields

$$\begin{aligned}
&\int \chi(\tau)p^{\mathrm{h}}(\tau)^2V'''(q^{\mathrm{h}}(\tau))\mathrm{d}\tau \\
&= \left(p^{\mathrm{h}}(t)^2V''(q^{\mathrm{h}}(t)) + \dot{p}^{\mathrm{h}}(t)^2\right)\int_0^t \frac{\mathrm{d}\tau}{p^{\mathrm{h}}(\tau)^2} - \int\left(V''(q^{\mathrm{h}}(\tau)) + \frac{\dot{p}^{\mathrm{h}}(\tau)^2}{p^{\mathrm{h}}(\tau)^2}\right)\mathrm{d}\tau \\
&= \left(p^{\mathrm{h}}(t)V''(q^{\mathrm{h}}(t)) + \frac{\dot{p}^{\mathrm{h}}(t)^2}{p^{\mathrm{h}}(t)}\right)\chi(t) + \frac{\dot{p}^{\mathrm{h}}(t)}{p^{\mathrm{h}}(t)}
\end{aligned}$$

via integration by parts, where we have used (3.7) and the equality

$$\frac{\mathrm{d}}{\mathrm{d}t}\left(\frac{\dot{p}^{\mathrm{h}}(t)}{p^{\mathrm{h}}(t)}\right) = \frac{\ddot{p}^{\mathrm{h}}(t)p^{\mathrm{h}}(t) - \dot{p}^{\mathrm{h}}(t)^2}{p^{\mathrm{h}}(t)^2} = -V''(q^{\mathrm{h}}(t)) - \frac{\dot{p}^{\mathrm{h}}(t)^2}{p^{\mathrm{h}}(t)^2}.$$

Let

$$\gamma_\pm = -\frac{V''(q_0)}{2\sigma_\pm} + \frac{\sigma_\pm^3}{2V''(q_0)} + \sigma_\pm,$$

where

$$\sigma_\pm = \lim_{t\to\pm\infty}\frac{\dot{p}^{\mathrm{h}}(t)}{p^{\mathrm{h}}(t)}.$$

Note that the limits $\sigma_\pm$ exist since $p^{\mathrm{h}}(t)$ tends to zero exponentially as $t \to \pm\infty$. Since

$$\lim_{t\pm\infty}\left(\left(p^{\mathrm{h}}(t)V''(q^{\mathrm{h}}(t)) + \frac{\dot{p}^{\mathrm{h}}(t)^2}{p^{\mathrm{h}}(t)}\right)\chi(t) + \frac{\dot{p}^{\mathrm{h}}(t)}{p^{\mathrm{h}}(t)}\right) = \gamma_\pm \tag{3.9}$$

as shown in Appendix, we obtain

$$\begin{aligned}
&-\int_t^\infty \chi(\tau)p^{\mathrm{h}}(\tau)^2V'''(q^{\mathrm{h}}(\tau))\mathrm{d}\tau + \gamma_+ \\
&= \int_{-\infty}^t \chi(\tau)p^{\mathrm{h}}(\tau)^2V'''(q^{\mathrm{h}}(\tau))\mathrm{d}\tau + \gamma_- \\
&= \left(p^{\mathrm{h}}(t)V''(q^{\mathrm{h}}(t)) + \frac{\dot{p}^{\mathrm{h}}(t)^2}{p^{\mathrm{h}}(t)}\right)\chi(t) + \frac{\dot{p}^{\mathrm{h}}(t)}{p^{\mathrm{h}}(t)}.
\end{aligned} \tag{3.10}$$

Substituting (3.8) and (3.10) into the first equation of (3.5), we compute

$$\begin{aligned}
&\tilde{q}^{\,\mathrm{s}}(t;\beta,\varepsilon) \\
&= \frac{1}{4}(\beta_1^2+\beta_2^2)\left(p^{\mathrm{h}}(t)\left(\left(p^{\mathrm{h}}(t)V''(q^{\mathrm{h}}(t)) + \frac{\dot{p}^{\mathrm{h}}(t)^2}{p^{\mathrm{h}}(t)}\right)\chi(t) + \frac{\dot{p}^{\mathrm{h}}(t)}{p^{\mathrm{h}}(t)} - \gamma_+ - \tilde{q}_0^{\mathrm{s}}\right)\right. \\
&\qquad \left. - \chi(t)\left(p^{\mathrm{h}}(t)^{2V''}(q^{\mathrm{h}}(t)) + \dot{p}^{\mathrm{h}}(t)^2\right)\right) \\
&= \frac{1}{4}(\beta_1^2+\beta_2^2)(\dot{p}^{\mathrm{h}}(t) - (\tilde{q}_0^{\mathrm{s}} + \gamma_+)p^{\mathrm{h}}(t)),
\end{aligned}$$

where the $O(\varepsilon)$-terms are ignored. Similarly, ignoring the $O(\varepsilon)$-terms and using the second equation of (3.5), we obtain

$$\tilde{q}^{\,\mathrm{u}}(t;\beta,\varepsilon) = \frac{1}{4}(\beta_1^2+\beta_2^2)(\dot{p}^{\mathrm{h}}(t) + (\tilde{q}_0^{\mathrm{u}} - \gamma_-)p^{\mathrm{h}}(t)).$$

Choosing $\tilde{q}_0^{\mathrm{s}} = -\gamma_+$ and $\tilde{q}_0^{\mathrm{u}} = \gamma_-$, we obtain the desired result. □

Using Lemma 3.1 and applying arguments in Sec. IV of Ref. 29 to (3.3), we prove the following.

Lemma 3.2. We have

$$d_0(t_0,\beta,\varepsilon) = \frac{\varepsilon M_0}{|(V'(q(t_0),p(t_0))|} + O(\varepsilon^2),$$
$$d_j(t_0,\beta,\varepsilon) = \frac{\varepsilon M_j}{|(\dot{p}^{\mathrm{h}}(t_0),p^{\mathrm{h}}(t_0))|} + O(\varepsilon^2), \quad j = 1,2,$$

where

$$M_0 = -\frac{1}{4}(\beta_1^2+\beta_2^2)\int_{-\infty}^{-\infty} p^{\mathrm{h}}(t)^3 V'''(q^{\mathrm{h}}(t))\mathrm{d}t,$$
$$M_j = \frac{1}{4}\beta_j(\beta_1^2+\beta_2^2)\int_{-\infty}^{\infty} p^{\mathrm{h}}(t)^2\dot{p}^{\mathrm{h}}(t)V'''(q^{\mathrm{h}}(t))\mathrm{d}t, \quad j = 1,2.$$

Proof. Let

$$\Delta_0^{\mathrm{s,u}}(t;\beta,\varepsilon) = \left(V'(q^{\mathrm{h}}(t)),p^{\mathrm{h}}(t)\right)\cdot\left(q^{\mathrm{h}}(t)+\varepsilon\tilde{q}^{\mathrm{s,u}}(t;\beta,\varepsilon),\ p^{\mathrm{h}}(t)+\varepsilon\tilde{p}^{\mathrm{s,u}}(t;\beta,\varepsilon)\right)$$

and

$$\Delta_j^{\mathrm{s,u}}(t;\beta,\varepsilon)$$
$$= \left(\dot{p}^{\mathrm{h}}(t),-p^{\mathrm{h}}(t)\right)\cdot\left(\beta_j p^{\mathrm{h}}(t)+\varepsilon\tilde{Q}_j^{\mathrm{s,u}}(t;\beta,\varepsilon),\ \beta_j\dot{p}^{\mathrm{h}}(t)+\varepsilon\tilde{P}_j^{\mathrm{s,u}}(t;\beta,\varepsilon)\right), \quad j = 1,2.$$

We have

$$d_0(t_0,\beta,\varepsilon) = \frac{\Delta_0^{\mathrm{u}}(t_0;\beta,\varepsilon)-\Delta_0^{\mathrm{s}}(t_0;\beta,\varepsilon)}{|(V'(q^{\mathrm{h}}(t_0)),p^{\mathrm{h}}(t_0))|}$$

and

$$d_j(t_0,\beta,\varepsilon) = \frac{\Delta_j^{\mathrm{u}}(t_0;\beta,\varepsilon)-\Delta_j^{\mathrm{s}}(t_0;\beta,\varepsilon)}{|(\dot{p}^{\mathrm{h}}(t_0),-p^{\mathrm{h}}(t_0))|}, \quad j = 1,2.$$

We see that

$$\frac{\partial}{\partial t}\Delta_0^{\mathrm{s,u}}(t;\beta,\varepsilon) = -\frac{1}{4}\varepsilon(\beta_1^2+\beta_2^2)p^{\mathrm{h}}(t)^3V'''(q^h(t)) + O(\varepsilon^2)$$

and

$$\frac{\partial}{\partial t}\Delta_j^{\mathrm{s,u}}(t;\beta,\varepsilon) = \frac{1}{4}\varepsilon\beta_j(\beta_1^2+\beta_2^2)p^{\mathrm{h}}(t)^2\dot{p}^{\mathrm{h}}(t)V'''(q^h(t)) + O(\varepsilon^2),$$

where we have used (3.3) and (3.4). Integrating the above equations from $t = t_0$ to ∞ or from $t = -\infty$ to t_0, we obtain

$$\Delta_0^{\mathrm{s}}(\infty;\beta,\varepsilon)-\Delta_0^{\mathrm{s}}(t_0;\beta,\varepsilon) = -\frac{1}{4}\varepsilon(\beta_1^2+\beta_2^2)\int_{t_0}^{\infty} p^{\mathrm{h}}(t)^3V'''(q^h(t))\mathrm{d}t + O(\varepsilon^2),$$
$$\Delta_0^{\mathrm{u}}(t_0;\beta,\varepsilon)-\Delta_0^{\mathrm{u}}(-\infty;\beta,\varepsilon) = -\frac{1}{4}\varepsilon(\beta_1^2+\beta_2^2)\int_{-\infty}^{t_0} p^{\mathrm{h}}(t)^3V'''(q^h(t))\mathrm{d}t + O(\varepsilon^2)$$

and

$$\Delta_j^{\mathrm{s}}(\infty;\beta,\varepsilon)-\Delta_j^{\mathrm{s}}(t_0;\beta,\varepsilon)$$
$$= \frac{1}{4}\varepsilon(\beta_1^2+\beta_2^2)\int_{t_0}^{\infty} p^{\mathrm{h}}(t)^2\dot{p}^{\mathrm{h}}(t)V'''(q^h(t))\mathrm{d}t + O(\varepsilon^2),$$
$$\Delta_j^{\mathrm{u}}(t_0;\beta,\varepsilon)-\Delta_j^{\mathrm{u}}(-\infty;\beta,\varepsilon)$$
$$= \frac{1}{4}\varepsilon(\beta_1^2+\beta_2^2)\int_{-\infty}^{t_0} p^{\mathrm{h}}(t)^2\dot{p}^{\mathrm{h}}(t)V'''(q^h(t))\mathrm{d}t + O(\varepsilon^2), \quad j = 1,2,$$

so that

$$\Delta_j^{\mathrm{u}}(t_0;\beta,\varepsilon)-\Delta_j^{\mathrm{s}}(t_0;\beta,\varepsilon) = \varepsilon M_j + O(\varepsilon^2), \quad j = 0,1,2,$$

since $\lim_{t\to-\infty}\Delta_j^{\mathrm{u}}(t;\beta,\varepsilon), \lim_{t\to\infty}\Delta_j^{\mathrm{s}}(t;\beta,\varepsilon) = 0$ for $j = 0,1,2$. Thus, we obtain the desired result. □

We immediately obtain Theorem 1.1 from the following proposition.

Proposition 3.3. Suppose that the integral (1.9) is not zero. Then the stable and unstable manifolds of the hyperbolic saddle (1.8) split outside of the (q,p)-plane, and their distance is $O(\varepsilon)$ in the directions (1.10) and (1.11), while it is at most $O(\varepsilon^2)$ in the direction (1.12).

Proof. We first note that $\beta \neq 0$ in the expressions (3.1) and (3.2) for the orbits on $W^{\mathrm{s}}_{\varepsilon}$ and $W^{\mathrm{u}}_{\varepsilon}$ outside of the (q,p)-plane. Using the relation (3.7), we compute

$$M_0 = -\frac{1}{4}(\beta_1^2+\beta_2^2)\left[p^{\mathrm{h}}(t)^2 V''(q^{\mathrm{h}}(t)) + \dot{p}^{\mathrm{h}}(t)^2\right]_{-\infty}^{\infty} = 0,$$

since both $p^{\mathrm{h}}(t)$ and $\dot{p}^{\mathrm{h}}(t)$ tend to zero as $t \to \pm\infty$. We notice by condition (1.9) that $M_j \neq 0$, $j = 1,2$, and use Lemma 3.2 to complete the proof. □

IV. EXAMPLE

In this section we illustrate our main result for the semiclassical system (1.6) with the potential (1.5), for which the classical system (1.4) is the simple pendulum. We also give some numerical results to demonstrate the theoretical result.

A. Separatrix splitting

We first apply Theorem 1.1 to show that separatrix splitting occurs in (1.6) with (1.5). Clearly, assumption (A1) holds for the potential (1.5). As in Fig. 2, we take $\mathbb{S}^1$ instead of $\mathbb{R}$ as the configuration space for the classical system (1.4) with (1.5), so that its phase space becomes $\mathbb{S}^1 \times \mathbb{R}$. See Fig. 4 for its phase portraits. In particular, there exists a hyperbolic saddle at $(q,p) = (\pi, 0)$ which has a pair of homoclinic orbits

$$(q^{\mathrm{h}}_{\pm}(t), p^{\mathrm{h}}_{\pm}(t)) = (\pm 2 \arcsin(\tanh t), \pm 2 \operatorname{sech} t). \tag{4.1}$$

Thus, assumption (A2) holds as well. Noting that $V'''(q^{\mathrm{h}}(t)) = -\sin q^{\mathrm{h}}(t) = \dot{p}^{\mathrm{h}}(t)$, we compute the integral (1.9) as

$$\int_{-\infty}^{\infty} p^{\mathrm{h}}_{\pm}(t)^2 \dot{p}^{\mathrm{h}}_{\pm}(t)^2 \mathrm{d}t = 16 \int_{-\infty}^{\infty} \operatorname{sech}^4 t \tanh^2 t \, \mathrm{d}t = \frac{64}{15}.$$

Applying Theorem 1.1, we show that the three-dimensional stable and unstable manifolds of the hyperbolic saddle at

$$(q,p,Q,P) = (\pi,0,0,0) \in \mathbb{S}^1 \times \mathbb{R} \times \mathbb{R}^2 \times \mathbb{R}^2$$

split in the semiclassical system (1.6) and the distance between them is $O(\varepsilon)$ outside of the (q,p)-plane in the six-dimensional phase space. Moreover, their distance is $O(\varepsilon)$ in the directions

$$(q,p,Q_1,Q_2,P_1,P_2) = (0,0,\pm\operatorname{sech} t_0 \tanh t_0, 0, \mp\operatorname{sech} t_0, 0)$$

and

$$(0,0,0,\pm\operatorname{sech} t_0 \tanh t_0, 0, \mp\operatorname{sech} t_0),$$

while it is at most $O(\varepsilon^2)$ in the direction

$$(\operatorname{sech} t_0 \tanh t_0, -\operatorname{sech} t_0, 0, 0, 0, 0)$$

near

$$\begin{aligned}(q,p,Q_1,Q_2,P_1,P_2) = (&\pm 2\arcsin(\tanh t_0), \pm 2\operatorname{sech} t_0, \pm 2\beta_1 \operatorname{sech} t_0,\\ &\pm 2\beta_2 \operatorname{sech} t_0, \mp 2\beta_1 \operatorname{sech} t_0 \tanh t_0, \mp 2\beta_2 \operatorname{sech} t_0 \tanh t_0)\end{aligned}$$

for any $t_0 \in \mathbb{R}$ and $\beta \in \mathbb{R}^2 \backslash \{0\}$.

To demonstrate this theoretical result, we numerically computed the stable and unstable manifolds of the saddle $(q,p,Q,P) = (\pi,0,0,0) \in \mathbb{S}^1 \times \mathbb{R} \times \mathbb{R}^2 \times \mathbb{R}^2$. Here we used a numerical approach explained in Refs. 13 and 27 with the assistance of the computer tool AUTO.[8] We show the numerical result for $\varepsilon = 0.1$ in Fig. 5. Figures 5(a) and 5(b) display the projections of their intersections with the section $\{q = 0, Q_2 = 1\}$ onto the (p, Q_1, P_1)- and (p, Q_1, P_2)-spaces, respectively, and Figs. 5(c) and 5(d) display their projections onto the (P_1, P_2)- and (p, Q_1)-planes, respectively. Note that $t = 0$ when $q^{\mathrm{h}}_{+}(t) = 0$. We observe that the stable and unstable manifolds split outside of the (q,p)-plane in Figs. 5(a)–5(c). Moreover, they split in the P_1- and P_2-directions but do not visibly in the p- and Q_1-directions, as shown in Figs. 5(a)–5(d). These observations agree with our theoretical prediction. Note that by Theorem 1.1 the splitting distance between the stable and unstable manifolds on the section $\{q = 0, Q_2 = 1\}$ is $O(\varepsilon)$ in the P_1- and P_2-directions but $O(\varepsilon^2)$ at most in the p- and Q_1-directions since $\dot{p}^{\mathrm{h}}_{+}(0) = 0$.

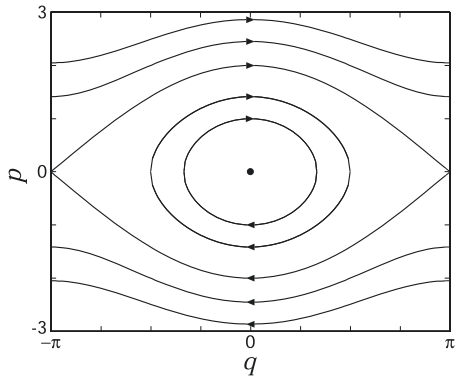

FIG. 4. Phase portraits of (1.4) with the potential (1.5).

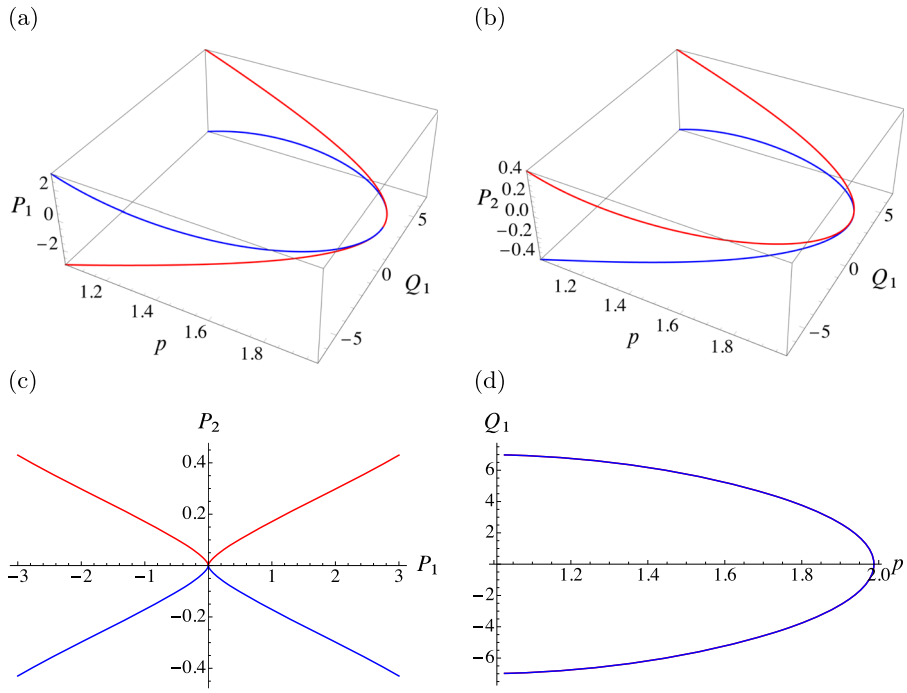

FIG. 5. Numerically computed stable and unstable manifolds of the hyperbolic saddle $(q, p, Q, P) = (\pi, 0, 0, 0) \in \mathbb{S}^1 \times \mathbb{R} \times \mathbb{R}^2 \times \mathbb{R}^2$ in the semiclassical system (1.6) with the potential (1.5) for $\varepsilon = 0.1$: (a) Projections of their intersections with the section $\{q = 0, Q_2 = 1\}$ onto the (p, Q_1, Q_2)-space; (b) onto the (p, Q_1, P_2)-space; (c) onto the (P_1, P_2)-plane; (d) onto the (p, Q_1)-plane. The stable and unstable manifolds are plotted as red and blue lines, respectively. Both projections almost completely coincide in (d).

B. Numerical solutions

Finally, we give some numerical solutions to the semiclassical system (1.6) with the potential (1.5) for $\varepsilon = 0.1$.

Figure 6 shows the intersection of the level set $H^\varepsilon = 1$ with the section $\{q = 0, Q_2 = 1, P_2 = 0\}$. The intersections of the numerically computed stable and unstable manifolds with the section $\{q = 0, Q_2 = 1\}$ onto the $\{p, Q_1, P_1\}$-space, which are displayed in Fig. 5, are also plotted in Fig. 6. We numerically solved (1.6) with (1.5) for $\varepsilon = 0.1$ on the time interval $[-5, 5]$ under four initial conditions at $t = 0$. The initial conditions were chosen to lie on the intersection of the level set $H^\varepsilon = 1$ with the section $\{(q, Q_2, P_2) = (0, 1, 0)\}$ near the stable and unstable manifolds, and to satisfy condition (1.3) (which reduces to $P_1 = -1$ given $(Q_2, P_2) = (1, 0)$). See Table I for their values of p and Q_1. In particular, the points labeled 1 and 3 (resp. 2 and 4) have the same value of p and are near the stable (resp. unstable) manifold. The point labeled 5 is the initial condition from Fig. 2. The five points are also labeled by the numerals 1–5 in Fig. 6.

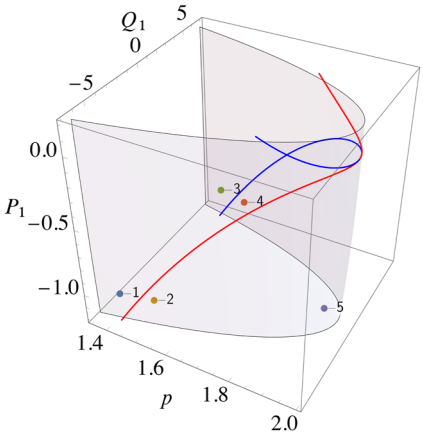

FIG. 6. Intersection of the level set $H^\varepsilon = 1$ with the section $\{q = 0, Q_2 = 1, P_2 = 0\}$ for $\varepsilon = 0.1$. The intersections of the numerically computed stable and unstable manifolds with the section $\{q = 0, Q_2 = 1\}$ displayed in Fig. 5 are also plotted as red and blue lines, respectively. The points labeled by the numerals 1–5 on the level set were used as the initial conditions of the numerical solutions to (1.6) with (1.5) plotted in Figs. 7–9.

TABLE I. The initial points of the numerical solutions displayed in Figs. 7–9. The values of Q_1 and H_0 are, respectively, provided to the fifth and fourth decimals places. The other values are $(q, Q_2, P_1, P_2) = (0, 1, -1, 0)$. These points are also plotted in Fig. 6.

label	p	Q_1	H_0
1	1.42	−6.137 75	0.0082
2	1.52	−5.638 44	0.1552
3	1.42	6.137 75	0.0082
4	1.52	5.638 44	0.1552
5	1.95	−1.396 42	0.9013

Figure 7 shows the (q, p)-components of the numerical solutions under the initial conditions labeled 1–5 in Fig. 6 and Table I. The solutions are labeled by the same numerals and plotted in the same color as the initial points. We observe that the solutions labeled 2 and 4 cross the separatrix both inward and outward while the solution labeled 1 (resp. 3) crosses the separatrix only inward (resp. outward). Since the projection of the stable (resp. unstable) manifold lies between the initial points labeled 1 and 2 (resp. 3 and 4) on the (Q_1, P_1)-plane, these manifolds seem to play a role of watersheds dividing whether a trajectory remain inside the separatrices or not. However, this statement is valid only when solutions stay near the manifolds. In fact, the (q, p)-components of the solution labeled 1 (resp. 3) were observed to eventually

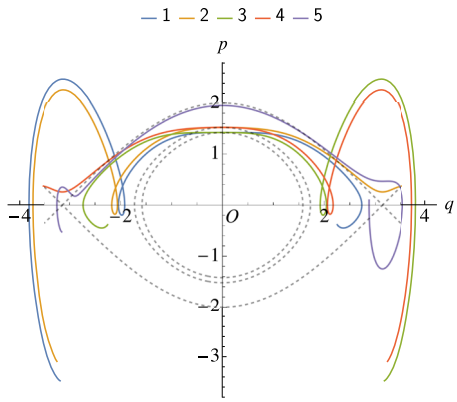

FIG. 7. The (q, p)-components of numerical solutions to the semiclassical system (1.6) with (1.5) for $\varepsilon = 0.1$ on the time interval $[-5, 5]$ under the initial conditions labeled 1–5 in Fig. 6 and Table I. The dashed curves are level sets of the classical Hamiltonian $H_0 = 0.0082, 0.1552, 1$. Here $H_0 = 1$ corresponds to the separatrices.

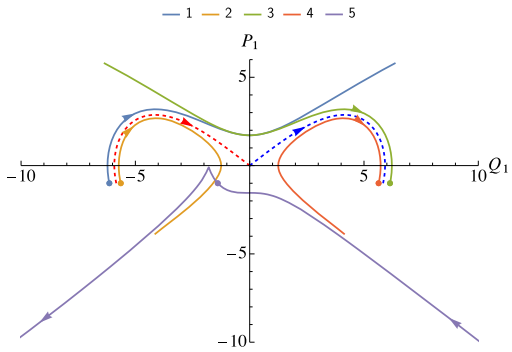

FIG. 8. The (Q_1, P_1)-components of numerical solutions to the semiclassical system (1.6) with (1.5) for $\varepsilon = 0.1$ under the initial conditions labeled 1–5 in Fig. 6 and Table I. The solutions are plotted on the time interval [0, 5] for 1 and 2, on $[-5, 0]$ for 3 and 4, and on $[-5, 5]$ for 5. The trajectories on the stable and unstable manifolds with the initial points on the section $\{q = 0, Q_2 = 1, P_1 = -1\}$ are plotted as the dashed red and blue lines, respectively.

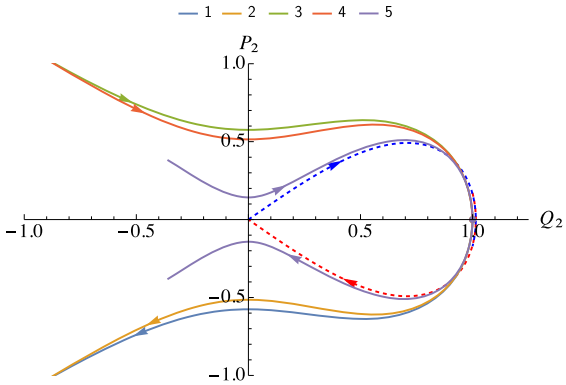

FIG. 9. The (Q_2, P_2)-components of numerical solutions to the semiclassical system (1.6) with (1.5) for $\varepsilon = 0.1$ under the initial conditions labeled 1–5 in Fig. 6 and Table I. The solutions are plotted on the time interval [0, 5] for 1 and 2, on $[-5, 0]$ for 3 and 4, and on $[-5, 5]$ for 5. The trajectories on the stable and unstable manifolds with the initial points on the section $\{q = 0, Q_2 = 1, P_1 = -1\}$ are plotted as the dashed red and blue lines, respectively.

cross the separatrix when $t \approx 5.69$ (resp. -5.69). The solution labeled 5 stays near the separatrix on the (q,p)-plane since its (q,p)-components are close to it at $t = 0$ (see Fig. 6) and the distance between them remains small on a time interval of $O(1)$.

Figures 8 and 9, respectively, show the (Q_1, P_1)- and (Q_2, P_2)-components of the numerical solutions under the initial conditions labeled 1–5 in Fig. 6 and Table I. The trajectories on the stable and unstable manifolds with the initial points on the section $\{q = 0, Q_2 = 1, P_1 = -1\}$ are also plotted as the dashed red and blue lines, respectively. We observe in Fig. 8 that the (Q_1, P_1)-components of the solutions labeled 1 and 2 (resp. 3 and 4) are separated by the trajectory on the stable (resp. unstable) manifold on the (Q_1, P_1)-directions, as in Fig. 7 for their (q,p)-components. The solution labeled 5 behaves very differently from these solutions since its initial point is very far from these manifolds (see Fig. 6). On the other hand, in Fig. 9, the (Q_2, P_2)-components of the solutions labeled 1 and 2 (resp. 3 and 4) cross the separatrix outward (resp. inward) on the (Q_2, P_2)-plane. However, the solutions labeled 1–4 behave very differently from the trajectories on the stable and unstable manifolds since the initial points are distinct between the former and latter: The latter are numerically estimated to cross the section $\{q = 0, Q_2 = 1, P_1 = -1\}$ at

$$(p, Q_1, P_2) \approx (1.482, -5.836, 0.1713) \quad \text{and} \quad (1.482, 5.836, -0.1713)$$

while the former cross the section at $P_2 = 0$ with the values (p, Q_1) given in Table I. The solution labeled 5 remains near the trajectories on the stable and unstable manifolds since its initial point is close to the separatrix except for the (Q_1, P_1)-components, which do not appear in the (Q_2, P_2)-components of (1.6).

ACKNOWLEDGMENTS

This work was partially supported by NSF Grant No. DMS-2006736 and the JSPS KAKENHI Grant No. JP22H01138.

AUTHOR DECLARATIONS

Conflict of Interest

The authors have no conflicts to disclose.

Author Contributions

Tomoki Ohsawa: Conceptualization (equal); Data curation (equal); Formal analysis (supporting); Funding acquisition (equal); Investigation (supporting); Methodology (supporting); Project administration (equal); Resources (equal); Software (supporting); Supervision (supporting); Validation (equal); Visualization (lead); Writing – original draft (supporting); Writing – review & editing (equal). **Kazuyuki Yagasaki**: Conceptualization (equal); Data curation (equal); Formal analysis (lead); Funding acquisition (equal); Investigation (lead); Methodology (lead); Project administration (equal); Resources (equal); Software (lead); Supervision (lead); Validation (equal); Visualization (supporting); Writing – original draft (lead); Writing – review & editing (equal).

DATA AVAILABILITY

The data that support the findings of this study are available from the corresponding author upon reasonable request.

APPENDIX: DERIVATION OF (3.9)

Using (2.2) and L'Hôpital's rule, we compute

$$\lim_{t\to\pm\infty} p^{\mathrm{h}}(t)\chi(t) = \lim_{t\to\pm\infty} \frac{\int_0^t \frac{\mathrm{d}t}{p^{\mathrm{h}}(t)^2}}{\frac{1}{p^{\mathrm{h}}(t)^2}} = -\lim_{t\to\pm\infty} \frac{\frac{1}{p^{\mathrm{h}}(t)^2}}{\frac{2\dot{p}^{\mathrm{h}}(t)}{p^{\mathrm{h}}(t)^3}} = -\frac{1}{2\sigma_\pm}. \tag{A1}$$

Moreover,

$$\begin{aligned}\lim_{t\to\pm\infty} \frac{\dot{p}^{\mathrm{h}}(t)^2}{p^{\mathrm{h}}(t)}\chi(t) &= \lim_{t\to\pm\infty} \frac{\int_0^t \frac{\mathrm{d}t}{p^{\mathrm{h}}(t)^2}}{\frac{1}{\dot{p}^{\mathrm{h}}(t)^2}} = -\lim_{t\to\pm\infty} \frac{\frac{1}{p^{\mathrm{h}}(t)^2}}{\frac{2\dot{p}^{\mathrm{h}}(t)}{\dot{p}^{\mathrm{h}}(t)^3}} \\ &= -\lim_{t\to\pm\infty} \frac{\dot{p}^{\mathrm{h}}(t)^3}{2p^{\mathrm{h}}(t)^2\ddot{p}^{\mathrm{h}}(t)} = \frac{\sigma_\pm^3}{2V''(q_0)}\end{aligned} \tag{A2}$$

by (3.6). Using (A1) and (A2), we obtain

$$\lim_{t\pm\infty}\left(\left(p^{\mathrm{h}}(t)V''(q^{\mathrm{h}}(t)) + \frac{\dot{p}^{\mathrm{h}}(t)^2}{p^{\mathrm{h}}(t)}\right)\chi(t) + \frac{\dot{p}^{\mathrm{h}}(t)}{p^{\mathrm{h}}(t)}\right) = -\frac{V''(q_0)}{2\sigma_\pm} + \frac{\sigma_\pm^3}{2V''(q_0)} + \sigma_\pm,$$

which yields (3.9).

REFERENCES

[1] Acosta-Humánez, P. B., Lázaro, J. T., Morales-Ruiz, J. J., and Pantazi, C., "Semiclassical quantification of some two degree of freedom potentials: A differential galois approach," J. Math. Phys. **65**(1), 012106 (2024).
[2] Albeverio, S., Gesztesy, F., Hoegh-Krohn, R., and Exner, P., *Solvable Models in Quantum Mechanics* (AMS Chelsea Publishing, 2005).
[3] Arnold, V., *Mathematical Methods of Classical Mechanics*, 2nd ed. (Springer, New York, 1989).
[4] Bouzouina, A. and Robert, D., "Uniform semiclassical estimates for the propagation of quantum observables," Duke Math. J. **111**(2), 223–252 (2002).
[5] Cartier, P. and DeWitt-Morette, C., *Functional Integration: Action and Symmetries* (Cambridge University Press, Cambridge, 2006).
[6] Combescure, M. and Robert, D., *Coherent States and Applications in Mathematical Physics* (Springer, Dordrecht, 2012).
[7] DeWitt-Morette, C., "The semiclassical expansion," Ann. Phys. **97**(2), 367–399 (1976).
[8] Doedel, E. and Oldeman, B., *AUTO-07P: Continuation and bifurcation software for ordinary differential equations*, 2012 available at http://cmvl.cs.concordia.ca/auto.
[9] Egorov, Y. V., "The canonical transformations of pseudodifferential operators," Uspekhi Mat. Nauk **24**(5), 235–236 (1969), https://www.mathnet.ru/eng/rm5554.
[10] Feynman, R. P. and Hibbs, A. R., *Quantum Mechanics and Path Integrals* (McGraw-Hill, New York, 1965).
[11] Hagedorn, G. A., "Semiclassical quantum mechanics. I. The $\hbar \to 0$ limit for coherent states," Commun. Math. Phys. **71**(1), 77–93 (1980).
[12] Hagedorn, G. A., "Raising and lowering operators for semiclassical wave packets," Ann. Phys. **269**(1), 77–104 (1998).
[13] van der Heijden, G. and Yagasaki, K., "Nonintegrability of an extensible conducting rod in a uniform magnetic field," J. Phys. A: Math. Theor. **44**, 495101 (2011).
[14] Heller, E. J., "Time-dependent approach to semiclassical dynamics," J. Chem. Phys. **62**(4), 1544–1555 (1975).
[15] Lasser, C. and Röblitz, S., "Computing expectation values for molecular quantum dynamics," SIAM J. Sci. Comput. **32**(3), 1465–1483 (2010).
[16] Lasser, C. and Lubich, C., "Computing quantum dynamics in the semiclassical regime," Acta Numer. **29**, 229–401 (2020).

[17] Lubich, C., *From Quantum to Classical Molecular Dynamics: Reduced Models and Numerical Analysis* (European Mathematical Society, Zürich, Switzerland, 2008).
[18] Miller, W. H., "Classical *S* matrix: Numerical application to inelastic collisions," J. Chem. Phys. **53**(9), 3578–3587 (1970).
[19] Miller, W. H., "Quantum mechanical transition state theory and a new semiclassical model for reaction rate constants," J. Chem. Phys. **61**(5), 1823–1834 (1974).
[20] Miller, W. H., "The semiclassical initial value representation: A potentially practical way for adding quantum effects to classical molecular dynamics simulations," J. Phys. Chem. A **105**(13), 2942–2955 (2001).
[21] Morales-Ruiz, J. J., *Differential Galois Theory and Non-Integrability of Hamiltonian Systems* (Birkhäuser, Basel, 1999).
[22] Morales-Ruiz, J. J., "A differential Galois approach to path integrals," J. Math. Phys. **61**, 052103 (2020).
[23] Morales-Ruiz, J. J. and Ramis, J.-P., "Galoisian obstructions to integrability of Hamiltonian systems," Methods Appl. Anal. **8**, 33–96 (2001).
[24] Morette, C., "On the definition and approximation of Feynman's path integrals," Phys. Rev. **81**(5), 848–852 (1951).
[25] Ohsawa, T., "Approximation of semiclassical expectation values by symplectic Gaussian wave packet dynamics," Lett. Math. Phys. **111**(5), 121 (2021).
[26] Ohsawa, T. and Leok, M., "Symplectic semiclassical wave packet dynamics," J. Phys. A: Math. Theor. **46**(40), 405201 (2013).
[27] Shibayama, M. and Yagasaki, K., "Heteroclinic connections between triple collisions and relative periodic orbits in the isosceles three-body problem," Nonlinearity **22**(10), 2377–2403 (2009).
[28] Wang, H., Sun, X., and Miller, W. H., "Semiclassical approximations for the calculation of thermal rate constants for chemical reactions in complex molecular systems," J. Chem. Phys. **108**(23), 9726–9736 (1998).
[29] Yagasaki, K., "The method of Melnikov for perturbations of multi-degree-of-freedom Hamiltonian systems," Nonlinearity **12**(4), 799–822 (1999).
[30] Yagasaki, K., "Semiclassical perturbations of single-degree-of-freedom Hamiltonian systems II: Nonintegrability," J. Math. Phys. **65**, 102707 (2024).
[31] Zworski, M., *Semiclassical Analysis* (American Mathematical Society, Providence, RI, 2012).